Seismic analysis of an isolated and a non-isolated light-frame timber building using artificial and natural accelerograms

L. SANCIN[1], G. RINALDIN[2], M. FRAGIACOMO[1] and C. AMADIO[2]

[1] Dept. of Architecture, Design and Urban Planning, University of Sassari, Alghero, Italy
[2] Dept. of Civil Engineering and Architecture, University of Trieste, Italy

ABSTRACT   Light-frame construction is used extensively for low and medium rise timber buildings. These buildings are light-weight and have a high dissipative capacity which, on the other hand, may imply significant structural and non-structural damage at the end of a high intensity earthquake ground motion, leading to potentially significant economic losses. Passive base isolation is by far the most effective way to reduce the effect of an earthquake on a structure. In this paper, the use of Friction Pendulum System isolators is investigated for a three-storey light-frame timber building. Two designs of the same building, with and without passive base isolation, were carried out according to Eurocodes 5 and 8 and the Italian technical regulation for construction. The buildings were then analysed using linear and non-linear methods. The seismic performance and cost of both solutions are compared, demonstrating the convenience of using passive base isolation.

Key words: timber building, light-frame construction, non-linear analysis, seismic design, passive base isolation.

1. Introduction

According to the modern philosophy of the Damage Avoidance Design (DAD) (Mander and Cheng, 1997; Bradley *et al*., 2008), a structure should be designed not only to survive a high intensity earthquake ground motion, but also to minimize the structural and non-structural damage. Passive base isolation is by far the most effective way to reduce the consequences of an earthquake on an existing or new structure (Zayas *et al*., 1990; Mezzi and Parducci, 1998). Its use has been somewhat limited by the cost, which is often believed to be high. However, significant progress has been made in this decade on passive base isolation, and nowadays the cost of this technique has markedly reduced. For these reasons, passive base isolation systems were recently used also for residential applications. For example, in L'Aquila (Italy) both reinforced concrete (RC) and timber buildings built after the 2009 earthquake were base isolated. The effectiveness of passive base isolation was demonstrated at length by the earthquakes occurred in Los Angeles in 1994 and in Kobe in 1995, where a dramatically different performance was observed in isolated and non-isolated buildings. It is therefore of interest to investigate this option also for timber buildings, where the significantly reduced

weight compared to RC allows the use of smaller and, therefore, potentially cheaper base devices. The paper explores the use of Friction Pendulum System (FPS) for light-frame multi-storey timber buildings. Two designs of a three-storey light-frame building were carried out according to Eurocodes 5 (EN 1995-1-1, 2004) and 8 (EN 1998-1, 2005) and the Italian regulation for construction (NTC2008, 2008): one with (Building B) and the other without isolators (Building A). The seismic performance and cost of both solutions are compared, demonstrating the advantage of passive base isolation.

2. Ductility in light-frame timber

Light-frame timber structures are composed by plywood or other types of sheathing nailed on light timber frames. It is well-known that the dissipative behaviour of a light-frame timber structure is mainly governed by the panel-to-frame connection in the first loading cycles. The collapse can occur for localised splitting of the wood or for connection failure, and it is brittle or ductile, respectively, in the two cases. In this respect it is of fundamental importance to evaluate the overstrength of the connection for the correct design of the connected wood elements. To obtain a ductile behaviour of the structure, the strength capacity of the ductile element must be smaller than the strength of the brittle element.

According to a correct design approach, the only dissipative elements in light-frame timber buildings are the panel-to-frame nailed connections of the shear walls (Beattie *et al.*, 2001; Follesa *et al.*, 2011). All other connections (hold-downs, tie-downs, angular brackets), all timber members (studs, plates, sheathing, joists), and the panel-to-joist connections of the floor diaphragms have to remain elastic and be designed for the overstrength of the dissipative elements. In this paper all timber elements and nailed panel-to-joist connections were designed for the overstrength of the panel-to-frame connections of the shear walls at the first floor. In particular, the nailed panel-to-frame connections of the shear walls were calculated at the first floor, where the strength demand due to seismic actions is larger, and reproduced at the upper floors, where the seismic forces decrease, in order to ensure plasticization only occurs at the first floor.

3. Case study building

The analysed structure is a three-story light-frame timber building with two symmetric modules, as can be seen in Fig. 1, connected to each other just at the foundation and at the roof level. The building is regular and was designed as strategic since it will host the headquarters of the fire brigade. It is situated in L'Aquila (Italy), 700 m above sea level, in a suburban zone. The building was designed with (Building B) and without passive isolation (Building A). Fig. 2 displays a cross-section of the Building B. The vertical load-bearing structure is made from light-frame shear walls with double Oriented Strand Board (OSB) sheathing nailed on both sides of the timber frame. The studs are spaced 60 cm centre to centre or less, and the walls are reinforced with additional studs where concentrated forces are applied. In the larger openings, the top plate is integrated with a lintel. The shear walls at the base are connected to the RC
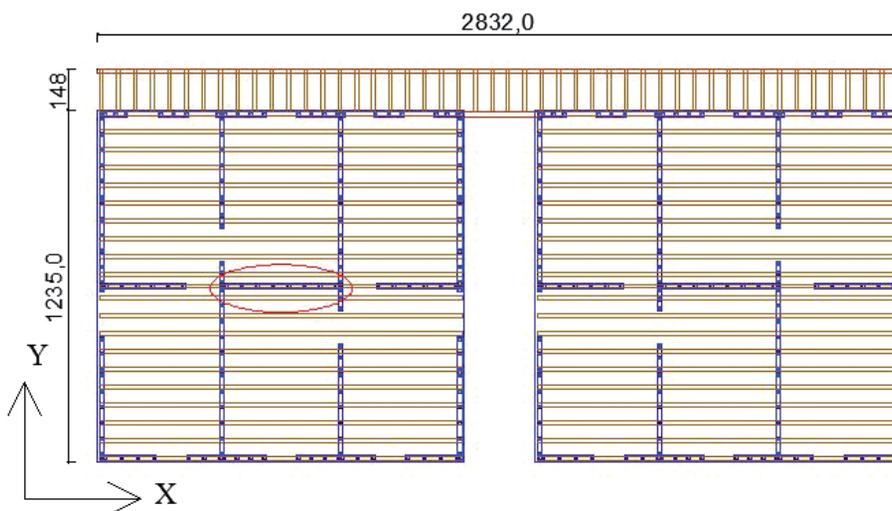
Fig. 1 - Plan view of the case study building. The results of the analysis for the circled wall are displayed in Fig. 11 (dimensions in cm).

ribbed slab with hold-downs and angle brackets, and to the upper walls with tie-downs and angle brackets. The structural flooring is made of two 15 mm thick OSB sheathings nailed on top and bottom of joists and blockings. The roof is double pitched, ventilated and covered with tiles. Walls and floor diaphragms ensure a box behaviour that can easily carry wind load and earthquake action.

The floor diaphragms and the roof are regarded as in-plane rigid as recommended by current codes of practice [NZS 3603 (1993) and Eurocode 8 (EN 1998-1, 2005)] and literature references (Beattie *et al.*, 2001) for timber floors with sheathings nailed on joists and solid blockings without significant openings. The light-frame shear walls provide the lateral load resisting system - each wall resists the lateral load in the direction parallel to its plane.

The main design data of the building are, according to the Italian regulation (NTC2008, 2008):
- permanent load on floors: $G_k = 1.85$ kN/m^2;
- permanent load on roof: $G_k = 1.60$ kN/m^2;
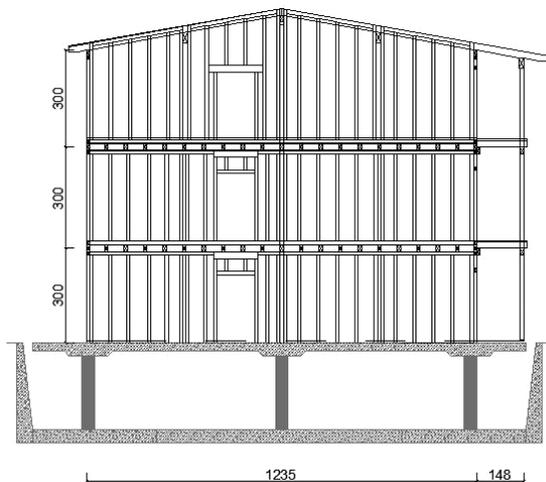
Fig. 2 - Cross-section of the isolated 3-storey light-frame building (dimensions in cm).

- imposed load on floors: $Q_k = 3$ kN/m² (office areas);
- snow load on the roof: $q_s = 1.27$ kN/m²;
- total drag load on windward and leeward facades: $q_w = 1.18$ kN/m²;
- reference service life: $V_r = 100$ yrs [which affects the design Peak Ground Acceleration (*PGA*)];
- site coordinates: 43.3660° N, 13.3944° E;
- ground type: B (deposits of very dense sand, gravel or very stiff clay, at least several tens of metres in thickness, characterised by a gradual increase of mechanical properties with depth);
- *PGA* for Collapse Limit State (CLS) seismic design: $a_g = 0.418$ *g*, *g* signifying the gravity acceleration;
- *PGA* for Life-safety Limit State (LLS) seismic design: $a_g = 0.331$ *g*;
- *PGA* for Damage Limit State (DLS) seismic design: $a_g = 0.142$ *g*;
- *PGA* for Operational Limit State (OLS) seismic design: $a_g = 0.113$ *g*;
- behaviour factor: $q = 4$ (Building A); $q = 1.5$ (Building B).

The load combination *F* for ULS (Ultimate Limit State) and SLS (Serviceability Limit State) design of the building subjected to the seismic actions is given by Eq. (1):

$$F = E + G_k + \psi_2 \cdot Q_k \qquad (1)$$

where $\psi_2 = 0.3$ for offices and *E* is the seismic action, calculated as a combination of the effects of the earthquake in X and Y directions ($\pm 1.00 \cdot E_x \pm 0.30 \cdot E_y$ or $\pm 1.00 \cdot E_y \pm 0.30 \cdot E_x$). E_x and E_y vary depending on the limit states, and are calculated proportionally to the seismic mass *M*, which is defined in the Italian regulation (NTC2008, 2008) according to Eq. (2):

$$M = (G_k + \psi_2 \cdot Q_k) / g \qquad (2)$$

The total seismic weight of the Building A is 4410 kN, while the seismic weight of the Building B superstructure is 4219 kN, that has to be added to the 3177 kN of the concrete ribbed slab supported by the isolators. According to the Italian regulation (NTC2008, 2008), strategic buildings have to satisfy the requirements of four different limit states: CLS, LLS, DLS and OLS. Every limit state has its own return period of the seismic event and thus the value of the design earthquake decreases going from the CLS to the OLS. In Table 1 the values of the base shear forces at the ground floor due to wind and earthquake [statically determined using NTC2008 (2008) spectra] in the different building directions are compared.

Table 1 - Comparison among base shear forces due to wind and earthquake.

Limit state	Building A		Building B	
	ULS (LLS)	DLS	ULS (LLS)	DLS
Wind X	281.8 kN		281.8 kN	
Wind Y	279.3 kN		279.3 kN	
Seismic action X	463.0 kN	718.8 kN	449.8 kN	207.3 kN
Seismic action Y	652.7 kN	1014.3 kN	432.2 kN	189.7 kN

4. Seismic isolation

After designing the Building A, the same building was re-designed with passive base isolation (Building B). The base floor diaphragm connecting the two modules of the building and supported by the isolation devices is made of a ribbed RC slab. The isolators are supported by stiff concrete columns connected to a flat plate foundation. In this way it is possible to obtain a basement that can be used as a garage, as typically required by architectural considerations. At the same time, according to the Italian regulation (NTC2008, 2008), the compulsory requirement of ensuring an easy maintenance and substitution of the isolation devices can be satisfied.

4.1. Friction pendulum system

Double Friction Pendulum System units (FPS) have been used in this paper as base isolation (Zayas *et al.*, 1990; Constantinou, 2004; Fenz and Constantinou, 2006). They are curved surface sliding isolators which exploit gravity for re-centring, like a pendulum. Dissipation of the input seismic energy takes place due to the friction on the main surface. The parameters of their cyclic behaviour depend on the curvature and on the friction coefficient. After the activation, the device develops a lateral force F_{din} that is given in Eq. (3) by the resultant of the dynamic friction force and the restoring force due to gravity:

$$F_{din} = \frac{W}{R} u + \mu_{din} W \qquad (3)$$

where F_{din} is the lateral force developed by the isolator in action; W is the weight of the timber superstructure and base floor diaphragm above the unit; μ_{din} is the dynamic friction coefficient; R is the radius of curvature of the isolator concave surface, and u is the isolator displacement.

The curvature radius is an important parameter in these system, as it governs the stiffness and therefore the natural vibration period of the isolated structure. The period T of a rigid mass supported by a FPS isolator can be calculated as in Eq. (4) (FIP Industriale, 2010):

$$T = 2\pi \sqrt{\frac{1}{g\left(\frac{1}{R} + \frac{\mu_{din}}{u_d}\right)}} \qquad (4)$$

where g is the gravity acceleration and u_d is the design displacement.

The equivalent lateral stiffness k_e of an active FPS isolator, relative to the maximum displacement u_{max}, is inversely proportional to the curvature radius R, as can be seen in Eq. (5) (FIP Industriale, 2010):

$$k_e = W\left(\frac{1}{R} + \frac{\mu_{din}}{u_{max}}\right) \qquad (5)$$

where the symbols have the same meaning as before. The direct proportion of the system stiffness to the weight bearing on it is fundamental for avoiding torsional problems in the

seismic response of the structure. In this way the stiffness centre coincides automatically with the mass centre.

4.2. Design of the isolators

The **Building B is designed for the same gravity and wind load as Building A, but the seismic** forces are smaller. Indeed, the isolation system was designed to obtain a natural vibration period T_1 = 2.93 s, corresponding to the final part of the design response spectrum, where the accelerations are less critical. As a result of that, the superstructure of **Building B is lighter, with** smaller cross-sections and with less nails required compared to Building A. A comparison for the most significant vibration periods and their mass participation ratios is shown in Table 2.

Table 2 - Comparison among vibration periods for fixed base (Building A) and isolated (Building B) and related mass participation ratios.

Building A			Building B		
T [s]	Direction	Participating mass ratio	T [s]	Direction	Participating mass ratio
1.00	X	90.0%	2.86	Y	99.7%
0.71	Y	82.7%	2.76	X	99.6%

The design of the isolators is carried out so as to comply with two performance requirements: i) the isolator should work (move) for the CLS and LLS design levels of earthquake ground motion; and ii) the isolator should behave like a fixed restraint for the design wind load at ultimate limit state. The first condition ensures that the isolators prevent any structural damage, according to the DAD philosophy. The second design condition is fundamental for the living comfort, as the wind occurs quite often and the waving motion of the isolators may cause seasickness of the occupants. Moreover, the continuous functioning of the isolators would lead to a major usury of the units and reduced safety level in the case of an earthquake. The displacement demand of the isolation system was calculated to be around 200 mm at CLS, so that the chosen device was a double curved surface FPS, with the following properties:
  • vertical load-carrying capacity: 1000 kN;
  • radius of the sliding surface: 2535 mm;
  • dynamic friction coefficient: 0.025;
  • maximum design displacement: 200 mm;
  • equivalent viscous damping coefficient (corresponding to the maximum design displacement): 15.3%;
  • natural period (corresponding to the maximum design displacement): 2.78 s
  • diameter (without anchorage): 430 mm;
  • depth (without anchorage): 89 mm.

The positioning of the FPSs is shown in Fig. 3. **The maximum distance between the devices** is almost 8 m. The limiting factor in deciding the maximum distance was the bending resistance of the concrete slab ribs and not the capacity of the isolation devices, which is much larger than
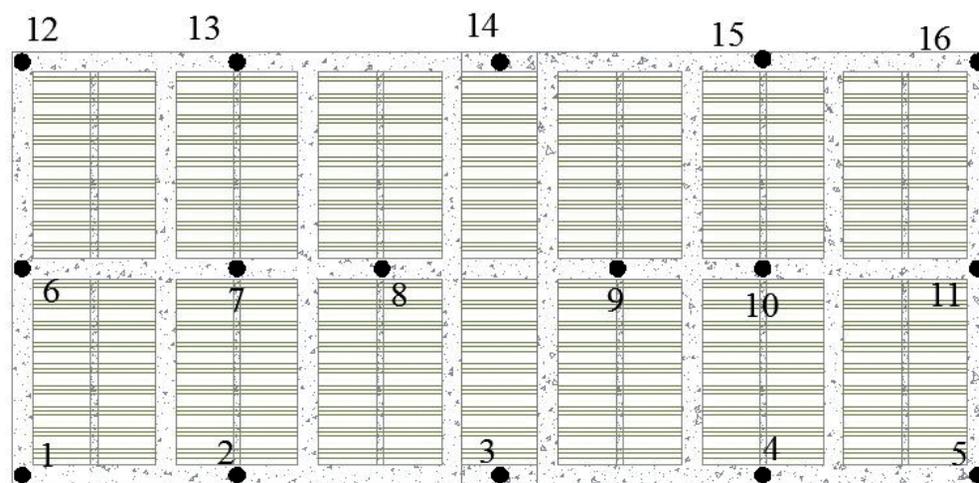
Fig. 3 - Positioning and labelling of the isolators.

necessary. The governing design conditions for the concrete slab ribs were sagging bending caused by gravity loads and also hogging bending at the supports due to the need to lift the beams about 1.5 cm for replacing the isolators at the end of their service life.

5. Numerical analysis

Some non-linear time-history analyses were performed with the aim to carry out a more accurate comparison of the seismic performance of both Buildings A and B. In these analyses, the seismic response of the structure is calculated by integration of the equation of motion using a non-linear model of the structure. The seismic action is represented by accelerograms that can be artificial, simulated or natural. Two approaches were used and compared: artificial accelerograms from SIMQKE-GR (2006) program and natural (recorded) accelerograms from Rexel program (Iervolino *et al*., 2012).

SIMQKE-GR (2006) is a software originally developed by the University of Berkeley that can generate, by superimposing sine waves, artificial accelerograms consistent with the desired design spectrum. The Rexel program (Iervolino *et al*., 2012) searches in a database a combination of seismic records, consistent with the desired design spectrum, selected according to the Italian seismic regulation or to Eurocode 8 (EN 1998-1, 2005). There are three databases included: the European Strong-motion Database (ESD), the Italian Accelerometric Archive (ITACA) made by the Italian National Institute for Geophysics and Volcanology (INGV), and the database containing the Selected Input Motions for displacement-Based Assessment and Design (SIMBAD). In this paper the accelerograms from ITACA database were used.

The SAP2000 (2011) non-linear finite element (FE) program, which is a software package widely used by practicing engineers, was employed to perform the analysis of the structure. Since the seismic performance of the whole building is markedly affected by the behaviour of the shear walls, careful consideration was given to the choice of a proper model which can effectively account for the most important features of the shear wall behaviour.

5.1. FE modelling of light-frame shear walls

The behaviour of light-frame timber shear walls is fairly complex as they are composed by different elements: timber frame, sheathing and connections (panel-to-frame nailed connection and anchoring of the wall to the foundation or to the floor underneath). All these elements contribute to the total flexibility of the wall, which affects the distribution of horizontal (seismic and wind) forces within the building. The need to model an entire three-storey building has suggested the opportunity to use a macro-model where all flexibility components are lumped together, rather than developing a computationally demanding schematization where all flexible elements (for example, each nail of the frame-to-panel connection) are explicitly modelled.
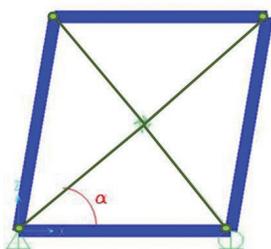
Fig. 4 - Deformed configuration of the macro-model of the shear wall under horizontal force applied on the top.

The macro-model is displayed in Fig. 4: it is made of uniaxial elements available in the SAP2000 (2011) library. More specifically, the two lateral studs (chords) and the top and bottom plates are modelled with rigid beam elements pinned to each other. The shear flexibility of the sheathing and the shear flexibility of the nailed panel-to-frame connection are modelled using two diagonal springs, with linear or cyclic behaviour [NLLink elements in SAP2000 (2011)], depending on the type of analysis (linear or non-linear) carried out. This macro-model has the advantage of simplicity and low computational demand, and is suitable for analyses of entire buildings. However, since the diagonal springs are fictitious elements, their mechanical properties need to be calibrated on experimental and analytical results to ensure that the behaviour of the macro-model is equivalent to that of a real shear wall.

The elastic axial stiffness K_{diag}, the yielding force $F_{y,diag}$ and the ultimate displacement $u_{ult,diag}$ of each diagonal can be calculated from simple geometrical considerations based on the elastic lateral stiffness $K=V/\Delta_w$, where V is the lateral force (total shear force) applied on top of the panel and Δ_w is the in-plane interstorey deflection of a light-frame shear wall loaded on top. It can be calculated using the formulas prescribed by the New Zealand Standard (NZS 3603, 1993) reported in Eq. (6):

$$\Delta_w = \Delta_4 + \Delta_5 + \Delta_6 + \Delta_7. \tag{6}$$

The four components of flexibility are displayed in Fig. 5.

Since the FE macro-model was used to model the cyclic behaviour of a shear wall in time-history analyses, the "Multi-linear plastic - Pivot Cycle" available in the SAP2000 (2011) library was chosen to schematize the hysteretic behaviour typically observed in light-frame shear walls. This relationship has been successfully employed in literature for another type of wooden
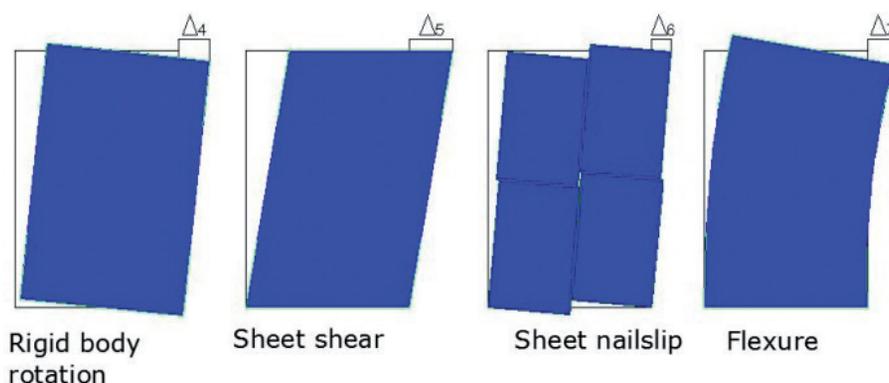
Fig. 5 - Deformation components of light-frame timber shear walls.

structure, in particular for modelling the connections in cross-laminated buildings (Fragiacomo and Rinaldin, 2011). The parameters needed to define the Pivot Cycle, namely the backbone curve and the variables α_1, α_2, β_1, β_2 for the setting of the unloading branches, were chosen by calibrating the hysteretic model on the experimental results of tests carried out at the University of Trieste in 2005 (Amadio *et al.*, 2007). Since the cycle is symmetric, only two parameters are needed: $\alpha_1 = \alpha_2 = 4.56$ and $\beta_1 = \beta_2 = 0.2$. The yielding force F_y was calculated according to Method A of Eurocode 5 (EN 1995-1-1, 2004), and the backbone curve was assumed as bi-linear. In Fig. 6 it can be seen the cyclic behaviour resulting from the numerical modelling with the Pivot Cycle, compared to the experimental results.

5.2. FE modelling of the buildings

The two Buildings A and B, with and without base isolation respectively, were modelled in SAP2000 (2011) to analyse their behaviour under seismic actions. Only the seismic resistant walls, schematized with the macro-model, were considered. The floor and roof diaphragms were regarded as in-plane rigid. In Building A the nodes of the walls were pinned-connected to the base. In Building B the concrete part (ribbed slab and stiff columns) and the isolators devices were added to the model. The cross sections of the walls were different and so was their stiffness. The FPS units were modelled using a particular non-linear spring (NLLink) of the SAP2000 (2011) library, called "Friction Isolator", which was calibrated on the stiffness and properties of the isolator resulting from the design.

These springs connect the concrete columns to the ribs of the supporting concrete slab, modelled with elastic beam elements. The columns are fixed to the base. The two models are shown in Figs. 7 and 8. The 3D models were used to carry out linear static, modal and non-linear time-history analyses.

For the time-history analysis, three artificial accelerograms generated with the program SIMQKE-GR ver. 4.0 (2006), consistent with the response spectrum calculated according to the Italian regulation for ground type B and different levels of *PGA* previously defined, were used as input. The same analysis was then performed again with seven natural accelerograms from Rexel ver. 3.3 beta (Iervolino *et al.*, 2012), consistent with the same design spectra.

The spectra of the used natural accelerograms from the ITACA database are shown in Fig. 9, compared to the target (design) spectrum for the LLS and DLS. The lower and the upper
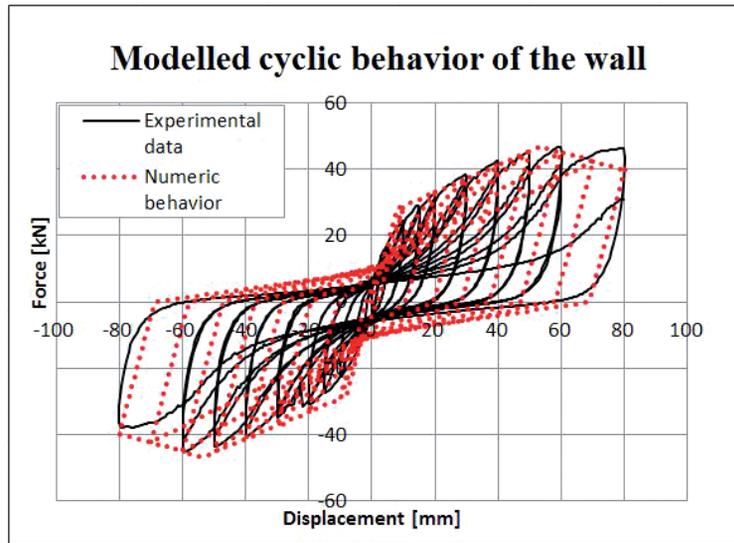
Fig. 6 - Comparison between numerical and experimental cyclic behaviour of a shear wall.

tolerance are 10% and 20% of the spectrum acceleration, respectively. The legend provides the wave code, the earthquake code and the scale factor of each record, which has been scaled in order to match the tolerances. The waveform code, the name of the earthquake, the date, the magnitude M_w, the fault mechanism of the accelerograms and the scale factors used for the analysis are listed in Table 3. In this table, the first block refers to the records used for LLS, whilst the second one is for DLS.

Some records in Table 3 are taken from the same seismic event. However, as can be noted from the legends of Fig. 9, some of them represent records from different stations around the epicentre of the same earthquake and thus they have different wave codes.

To use a ground motion with the closest characteristics of the real earthquakes that may occur in the site of the analysed building, only the records from the earthquakes of the same intensity
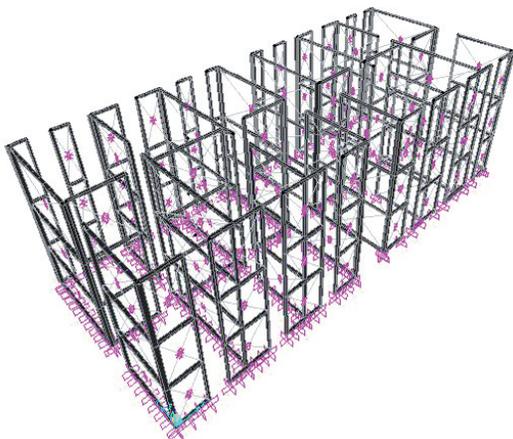
Fig. 7 - 3D view of the FE model of the Building A.
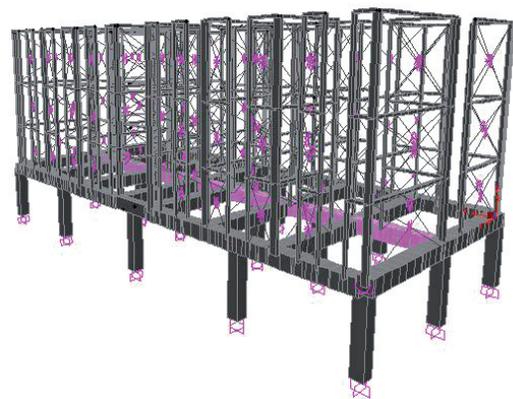
Fig. 8 - 3D view of the FE model of the Building B.
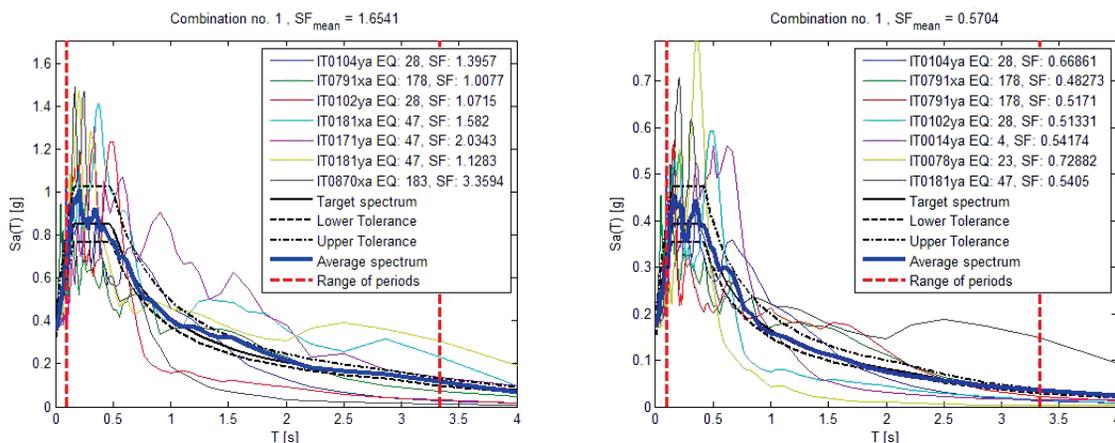
Fig. 9 - Spectra of the seven accelerograms used for the analysis, and comparison with the design spectrum for LLS (left) and DLS (right) limit state and its tolerance band.

Table 3 - Information about the earthquake events to which recorded accelerograms belong.

Waveform ID	Earthquake ID	Earthquake Name	Date	Mw	Fault Mechanism	Scale Factor
104	28	Friuli Earthquake 4th Shock	15/09/1976	5.9	Thrust	1.3957
791	178	L'Aquila Mainshock	06/04/2009	6.3	Normal	1.0077
102	28	Friuli Earthquake 4th Shock	15/09/1976	5.9	Thrust	1.0715
181	47	Irpinia Earthquake	23/11/1980	6.9	Normal	1.582
171	47	Irpinia Earthquake	23/11/1980	6.9	Normal	2.0343
181	47	Irpinia Earthquake	23/11/1980	6.9	Normal	1.1283
870	183	L'Aquila Earthquake	06/04/2009	5.6	Normal	3.3594
104	28	Friuli Earthquake 4th Shock	15/09/1976	5.9	Thrust	0.66861
791	178	L'Aquila Mainshock	06/04/2009	6.3	Normal	0.48273
791	178	L'Aquila Mainshock	06/04/2009	6.3	Normal	0.5171
102	28	Friuli Earthquake 4th Shock	15/09/1976	5.9	Thrust	0.51331
14	4	Friuli Earthquake 1st Shock	06/05/1976	6.4	Thrust	0.54174
78	23	Friuli Earthquake 2nd Shock	11/09/1976	5.6	Thrust	0.72882
181	47	Irpinia Earthquake	23/11/1980	6.9	Normal	0.5405

of the zone were selected. More specifically, only the records coming from the same type of ground (type B) were chosen. Also two accelerograms from the earthquakes occurred in 2009 in L'Aquila were used, one from the main shock and the other from the strongest secondary shock.

The behaviour of the two buildings was compared in terms of stresses in the elements, inter-storey drifts and floor accelerations, demonstrating the superior performance of the Building B. The time-history of the inter-storey drift resulting from the non-linear time-history analysis showed that the maximum inter-storey drift in Building B was much lower than in Building A. All the displacement demand is concentrated at the isolation interface, as can be seen in Fig. 10 for the

CLS, where it reaches 145 mm. The same figure demonstrates that the isolator worked (moved) also at DLS, providing protection to the building even for lower intensity earthquake ground motions. For the sake of completeness, Table 4 reports the resultant interstorey drift (for a seismic record applied with 100% intensity in X direction and 30% intensity in Y direction) and the maximum floor acceleration in X direction for the generated seismic input at DLS, LLS and CLS.
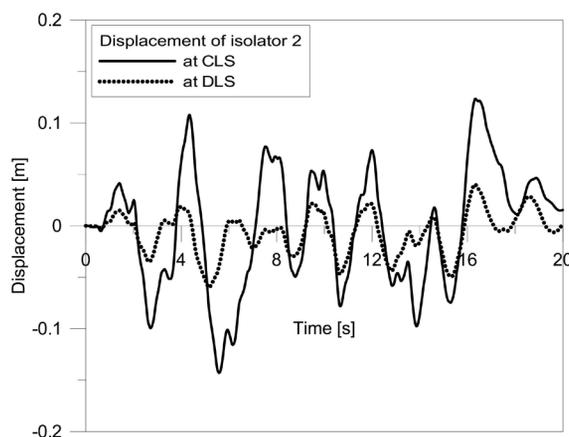
Fig. 10 - Displacement in one of the isolating devices (No. 2) for the CLS and DLS seismic levels, calculated with a generated accelerogram (total duration: 20 s).

Table 4 - Interstorey drifts and floor accelerations at different LS.

		Interstorey Drift [mm]			Acceleration [units of g]		
	Floor	DLS	LLS	CLS	DLS	LLS	CLS
Building A	1	13.93	60.1	98.3	0.211	0.457	0.479
	2	13.05	16.7	19.5	0.251	0.439	0.499
	3	10.74	13.2	16.24	0.418	0.476	0.516
Building B	1	4.14	5.03	5.22	0.048	0.070	0.085
	2	3.41	4.43	4.95	0.062	0.083	0.098
	3	2.63	3.62	3.9	0.077	0.103	0.124

The better performance demonstrated by the Building B is evident not only in terms of displacement but also in terms of accelerations, which are dramatically reduced in the building, with significant benefits for the content, secondary elements and occupants. Fig. 11 displays the force-displacement hysteresis loops in a timber shear wall (see the circled wall in Fig. 1) of the Building A at the 2nd and ground floor, for DLS. For the sake of clarity, the responses of only the ground motions producing the worst effects on the structure are displayed: two natural accelerograms (IT0014ya and IT0104ya) from Rexel, and one artificial from SIMQKE-GR (2006). The significant inter-storey drift demand causes the plasticization of the timber shear walls, especially at the ground floor. On the contrary, all the timber shear walls of the Building B remain elastic. These curves are not displayed in the figures because the total force in both walls is only 1/13 of the value in Building A case.
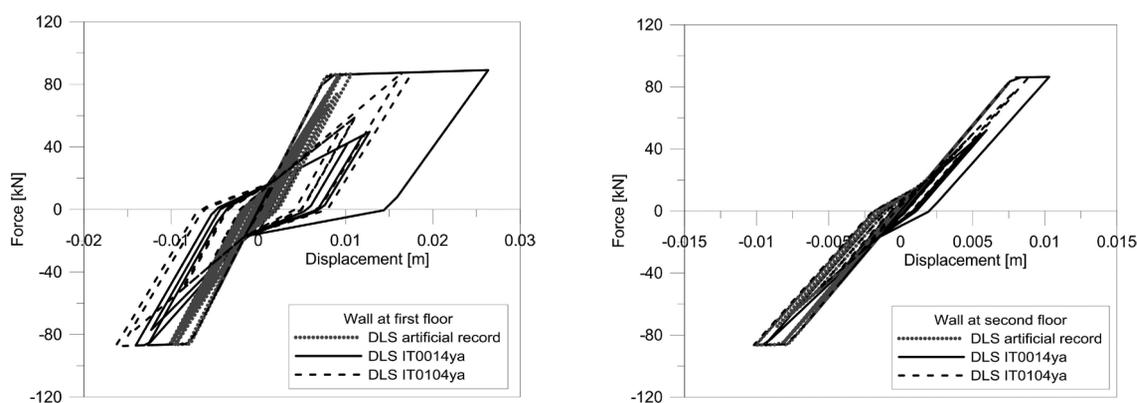
Fig. 11 - Hysteresis cycles of the reference shear wall at the ground floor (left) and at the 2nd floor (right) for DLS seismic action in Building A (results for artificial and recorded accelerograms).

6. Discussion

By designing separately the Buildings A and B and comparing the result of the designs, it was found that the timber superstructure of the Building B can be less strong and less stiff. The cross-section of studs in the walls of the isolated superstructure can be reduced by 33% (see Table 5). Although this reduction in volume is not significant, it helps cover part of the additional cost of isolators. The behaviour of the two structures, however, is markedly different. In Building B, the damage is avoided also for strong seismic events as the timber superstructure behaves elastically. Since the structural accelerations are very low, the panic of the occupants and the damage to the content of the building are prevented. This is a desirable feature particularly for strategic buildings such as hospitals, schools, laboratories, etc. where the value of the content is high, but also for commercial buildings hosting banks, insurance offices, etc. where the downtime due to the need of repairing and retrofitting the building following a strong earthquake ground motion should be limited as it would lead to significant economic losses. Although not explicitly required by current codes of practice such as the Eurocode, the Italian and New Zealand regulations, the use of passive base isolation in residential buildings has notably advantages, both economical and psychological, as it reduces the traumatic effects of an earthquake on the occupants, and avoids injures due to falling objects and debris.

Table 5 - Comparison between the isolated and non-isolated structure.

	Non-isolated structure	Isolated structure
Cross-section of studs and plates	12 cm × 16 cm	8 cm × 16 cm
No. of nails in hold-downs	45	24
No. of nails in angle brackets	21	15
Nail spacing in panel-to-frame connection	100 mm	150 mm

7. Costs comparison

In this section, a brief evaluation of the total cost for both structures (isolated and non-isolated) is presented. All costs are calculated starting from the prices provided by producers and manufacturers. The costs have been calculated assuming that both buildings have the same basement.

The main differences in Table 6 are represented by the structural material costs and by the cost of isolators. The cost of the concrete columns and slab supporting the timber structure including the finishes is considered in both the Buildings A and B. In Building B the total volume of the timber structure is less than in Building A, but more concrete has to be used to strengthen the ribbed RC slab supporting the timber superstructure above the isolators. In the end, however, the total cost of the two buildings differs by only 0.75%, which makes the use of passive base isolation for light-frame construction very attractive considered the superior performance of the Building B.

Table 6 - Cost comparison between the Buildings A and B.

Description	Building A	Building B
Wooden structure and finishes including labour cost	€ 745 467	€ 702 336
Concrete structure and finishes including labour cost	€ 399 802	€ 425 652
Installations	€ 216 578	€ 216 578
Windows and doors	€ 102 024	€ 102 024
Isolators	n.a.	€ 28 320
TOTAL	€ 1 463 871	€ 1 474 910

8. Conclusions

Timber buildings are widely used around the world. They are a sustainable construction system and, if well designed and built, they are suitable for seismic-prone areas due to their low mass. As wood structures are becoming more common also in countries with seismic hazard such as Italy, it is important to understand their seismic behaviour and design them to prevent, or limit, the damage.

In this paper the case study of a 3-storey light-frame timber building was investigated. Light-frame timber construction systems have a high dissipative capacity [a behaviour factor up to 5 is suggested by Eurocode 8 (EN 1998-1, 2005)], due to the many nailed connections between plywood or other type of sheathing and the light timber frames. This means that during a high intensity earthquake the structure is safe, but undergoes significant damage. The paper investigates the possibility of using passive base isolation for preventing this damage.

A three-storey light-frame building was first designed without and then with a seismic base isolation obtained using Friction Pendulums Isolators. The two buildings were modelled using the commercial FE program SAP2000 (2011) and then three seismic analyses were performed: a linear static, a modal and a non-linear time history analysis with both artificial and recorded

accelerograms. A research was undertaken to find the most suitable schematization of the light-frame shear-walls, as they are the elements that govern the seismic behaviour of the entire building. The parameters for modelling the shear-walls were calculated based on prescriptions from Eurocode 5 (EN 1995-1-1, 2004) and New Zealand Timber Standard.

Both the Buildings A and B were in-line with the seismic requirements of current regulations. Despite this, during the design earthquake the Building A undergoes high damage, especially at the ground floor, which is designed to dissipate the seismic energy. Conversely, the isolated structure remains elastic. The whole displacement is concentrated in the isolation units, which dramatically reduce the accelerations in the superstructure and satisfy the requirements of the DAD.

As the timber superstructure is very light compared to the vertical capacity of the isolators, the system is optimized if the timber superstructure is higher than two storeys and has a smaller area in plan. For the case study building analysed in this paper, where 16 isolators were used, it was calculated that the cost difference with the Building A is only 11,000 €, corresponding to 0.75% of the total cost of Building A. The factors that influence this difference are three: the saving in wood material for the isolated structure; the higher cost of the concrete basement for the isolated structure; and the cost of the isolating units. The additional cost of the isolation is by far counterbalanced by the increased safety of the building. Therefore, passive base isolation should be considered more often when designing light-frame timber buildings in earthquake-prone areas. Passive base isolation not only makes the buildings safer, but also dramatically improves the seismic performance of the structure during the earthquake, and consequently reduces fear of the occupants. However, particular care in reducing the cross sections of the structural elements has to be taken in Building B, in order to avoid excessive deformability or vibrations in the structure during the normal use. In this work, all the verifications required according to Eurocode 5 (EN 1995-1-1, 2004) and 8 (EN 1998-1, 2005) and the Italian technical regulation for construction have been done and the structure in Building B is not affected by this problem. Nevertheless, it should be observed that passive base isolation can be used only when the design is governed by seismic actions and not by wind actions, which is not always the case for timber buildings.

REFERENCES

Amadio C., Gattesco N. and Urban F.; 2007: *Indagine sperimentale su pareti di controvento in legno realizzate con pannelli in OSB o in gesso rinforzato con fibre*. In: Proc. XII Convegno ANIDIS, L'ingegneria sismica in Italia, Pisa, Italy, pp. 1-11, (in Italian).

Beattie G., Buchanan A.H., Gaunt D. and Soja E.; 2001: *Multi-storey timber buildings manual*. Carter Holt Harvey Wood Products, Fletcher Challenge Forests Ltd, James Hardie Building Products Inc. and Winstone Wallboards Ltd, Australia-New Zealand.

Bradley B.A., Dhakal R.P., Mander J.B. and Li L.; 2008: *Experimental multi-level seismic performance assessment of 3D RC frame designed for damage avoidance*. Earthquake Eng. Struct. Dyn., **37**, 1-20.

Constantinou M.C.; 2004: *Friction pendulum double concave bearing*. Technical Report, University at Buffalo, State University of New York, Buffalo, NY, USA, 33 pp. and 2 appendices.

EN 1995-1-1; 2004: *Eurocode 5: design of timber structures - Part 1-1: general - common rules and rules for buildings*. European Committee for Standardition (CEN), Bruxelles, Belgium, 123 pp. with EN 1995-1-1/AC: 2006 incorporated

EN 1998-1; 2005: *Eurocode 8: design of structures for earthquake resistance - Part 1: general rules seismic actions and rules for buildings*. European Committee for Standardition (CEN), Bruxelles, Belgium, 215 pp.

Fenz D.M. and Constantinou M.C.; 2006: *Behaviour of the double concave friction pendulum bearing*. Earthquake Eng. Struct. Dyn., **35**, 1403-1424.

FIP Industriale; 2010: *Catalogue S04. Isolatori a scorrimento a superficie curva*. Fip Group, Selvazzano Dentro, Padova, Italy, 15 pp., in Italian.

Follesa M., Fragiacomo M. and Lauriola M.P.; 2011: *A proposal for revision of the current timber part (Section 8) of Eurocode 8 - Part 1*. In: Proc. 44th Meeting Working Commission W18 - Timber Structures, CIB, Int. Council Res. Innov. Building Constr., Alghero, Italy, paper CIB-W18/44-15-1.

Fragiacomo M. and Rinaldin G.; 2011: *Advanced models for seismic analyses of timber buildings*. In: Außergewöhnliche Einwirkung - Erdbeben - im Holzbau, Workshop on crosslam construction "Grazer Holzbau-Fachtagung - 9. Gra FHT'11", Technical University of Graz, Austria, 30 pp.

Iervolino I., Galasso C. and Cosenza E.; 2012: *REXEL: computer aided record selection for code-based seismic structural analysis*. Bull. Earthquake Eng., **8**, 339-362.

Mander J.B. and Cheng C.T.; 1997: *Seismic resistance of bridge piers based on damage avoidance design*. Tech. report NCEER-97-0014, U.S. Nat. Center Earthquake Eng. Res. (NCEER), Dept. Civil Environ. Eng., Buffalo, NY, USA, 144 pp.

Mezzi M. and Parducci A.; 1998: *Base isolation in retrofitting historic buildings*. In: Proc. of Monument-98, Workshop on Seismic Performance of Monuments, Lisboa, Portugal, pp. 249-257.

NTC2008; 2008: *D.M. 14/01/2008 - Nuove norme tecniche per le costruzioni - NTC2008*. Consiglio Superiore dei Lavori Pubblici, Roma, Italy, in Italian.

NZS 3603; 1993: *Timber structures standard*. Wellington, New Zealand.

SAP2000; 2011: *Integrated* solution *for structural analysis & design, vers. 14.0.0, structural analysis program*. Computers and Structures Inc., Berkeley, CA, U.S.A.

SIMQKE-GR; 2006: *Programma per la generazione di accelerogrammi artificiali spettro-compatibili* vers. 4.0, *civil engineering free software*. Università di Brescia, Italy, http://dicata.ing.unibs.it/gelfi/software/programmi_studenti.html.

Zayas V.A., Low S.S. and Mahin S.A.; 1990: *A simple pendulum technique for achieving seismic isolation*. Earthquake Spectra, **6**, 317-333.

Corresponding author: Ljuba Sancin
Contemporary Building Design d.o.o.
Sojerejeva ulica 3, 1000 Ljubljana, Slovenia
Phone: +39 340 2741972; e-mail: ljuba.sancin@gmail.com